

The orbit of the double-lined Wolf-Rayet Binary HDE 318016 (= WR 98)

Roberto C. Gamen¹, Virpi S. Niemela²

Facultad de Ciencias Astronómicas y Geofísicas, Universidad Nacional de La Plata, Paseo del bosque s/n, B1900FWA La Plata, Argentina

Abstract

We present the discovery of OB type absorption lines superimposed to the emission line spectrum and the first double-lined orbital elements for the massive Wolf-Rayet binary HDE 318016 (=WR 98), a spectroscopic binary in a circular orbit with a period of 47.825 days. The semiamplitudes of the orbital motion of the emission lines differ from line to line, indicating mass ratios between 1 and 1.7 for $\mathcal{M}_{WR}/\mathcal{M}_{OB}$.

Key words: stars: binaries, stars: individual: (HDE 318016 = WR 98), stars: Wolf-Rayet

PACS: 97.30.Eh 97.80.Fk

1 Introduction

HDE 318016 was discovered to have an emission line spectrum of Wolf-Rayet type by Cannon & Mayall (1938). Because both N and C emission lines appear strong in the spectrum it was classified as WC7-N6 by Smith (1968). This star was included in the Sixth Catalogue of Galactic Wolf-Rayet Stars (van der Hucht et al. 1981) as WR 98 and classified as WN7+WC7. However WR 98 was confirmed to be a single-lined binary with a period of 47.8 days with N and C emission lines moving in phase (Niemela 1991).

The optical spectrum of WR 98 has been described by Lundström & Stenholm (1984). Conti & Massey (1989) proposed the nomenclature WN/WC for WR 98

¹ Fellow of CONICET, Argentina. Visiting Astronomer, CASLEO, San Juan, Argentina. E-mail: rgamen@fcaglp.unlp.edu.ar

² Member of Carrera del Investigador, CIC, BA, Argentina. Visiting Astronomer, CTIO, NOAO, operated by AURA, Inc., for NSF. Visiting Astronomer, CASLEO, San Juan, Argentina. E-mail: virpi@fcaglp.unlp.edu.ar

suggesting that this star, along with others with similar emission line spectra where both N and C lines are observed, has a transition composition between the WN and WC subclasses.

Smith et al. (1996) classified WR 98 as WN8o/C7, using a new three-dimensional classification scheme, where the “o” means that no hydrogen is observed in the spectrum. Relevant parameters of WR 98 can be found in the recent VIIth Catalogue of galactic WR stars (van der Hucht 2001).

WR 98 is a probable member of the open cluster Trumpler 27 (e.g. Feinstein et al. 2000), and it has also been detected as a non-thermal radio source by Abbott et al. (1986). Furthermore, WR 98 exhibits random relatively large amplitude optical light variations (~ 0.1 magnitude in the Johnson V filter), typical of stars with WN8 type spectrum, but a periodicity for these variations has not been found (Marchenko et al. 1998).

In this work we present a detailed radial velocity analysis of optical spectral lines of WR 98 showing it to be a double-lined binary with high minimum masses.

2 Observations

2.1 *Photographic spectra*

41 photographic spectrograms were obtained at the Cerro Tololo Inter-American Observatory, Chile, between 1980 and 1984. These spectrograms were secured with the image-tube spectrograph at the Cassegrain focus of the 1-m Yale telescope. All exposures were made on Kodak IIIa-J emulsion baked in “forming gas” ($N_2 + H_2$). The spectrograms have a reciprocal dispersion of 45 \AA mm^{-1} . A spectral region from ~ 3600 to 5000 \AA was covered. Exposure times vary between thirty and ninety minutes, giving Signal to Noise (S/N) ratios ~ 15 – 30 . A He-Ar lamp spectrum was used as wavelength calibration source.

A preliminary report of the binary nature of WR 98 based on these data was presented in the IAU Symp. 143 (Niemela 1991).

2.2 *Digital spectra*

28 optical digital spectral images of WR 98 were obtained with the Cassegrain Boller & Chivens (B&C) and REOSC spectrographs attached to the 2.15-m

telescope at Complejo Astronómico El Leoncito (CASLEO)³ in San Juan, Argentina, between 1997 and 2001. Nine spectra were secured with the B&C spectrograph, in 1997, March, and 1998, February and May. A PM 512×512 pixels CCD, with pixel size of 20μm, was used as detector. The reciprocal dispersion was $\sim 2.3 \text{ \AA pixel}^{-1}$, and the wavelength region covered was about $\lambda\lambda 3900 - 4900 \text{ \AA}$.

Nineteen spectra were obtained with the REOSC spectrograph, between 1999, March, and 2001, October. For these spectra a TEK 1024×1024 pixels CCD, with pixel size of 24μm, was used as detector. The reciprocal dispersion was $\sim 1.6 \text{ \AA pixel}^{-1}$, and the observed wavelength region was $\sim \lambda\lambda 3850 - 5450 \text{ \AA}$.

We used a slit width of 2 arcsecs for all our spectra. Typical exposure times for the stellar images were between 30 and 40 minutes, resulting in spectra of signal-to-noise ratio $S/N \sim 50-100$.

He-Ar (or Cu-Ar with REOSC spectrograph) comparison arc images were observed at the same telescope position as the stellar images immediately after or before the stellar exposures. Also bias and flat-field frames were obtained each night, as well as flux and radial velocity standard stars.

All spectra were processed with IRAF⁴ routines at La Plata Observatory.

2.3 Determination of radial velocities

Radial velocities of lines in the photographic spectra of WR 98 were measured with the Grant oscilloscope comparator–microphotometer at the Instituto de Astronomía y Física del Espacio (IAFE), Buenos Aires, Argentina.

For the present study, selected photographic spectrograms and their corresponding calibrations were digitized with a Grant microphotometer, and calibrated and measured with IRAF routines.

The emission lines in the spectrum of WR 98 appear approximately gaussian in shape (cf. Fig 1). Therefore, for determination of radial velocities in our digital spectra, we measured central wavelengths of all emission lines fitting gaussian functions to the line profiles.

The journal of the spectroscopic observations with the radial velocity measurements is presented in Table 1, where successive columns quote: the Heliocentric

³ operated under agreement between CONICET, SeCyT, and the Universities of La Plata, Córdoba and San Juan, Argentina

⁴ IRAF is distributed by the NOAO, operated by the AURA, Inc, under cooperative agreement with the NSF, USA.

Julian Date of each observation, the orbital phase, and the radial velocities for NIV, NV, CIII, HeII emission lines and H δ and H γ absorption lines, respectively.

Table 1: Observed heliocentric radial velocities (in km s⁻¹) in the spectra of WR 98

HJD	Phase ¹	N IV em. λ_0 4057.76	N V em. λ_0 4603.73	C III em. λ_0 4648.83	He II em. λ_0 4685.68	H γ abs. λ_0 4340.47	H β abs. λ_0 4861.33
44387.850	0.057		52	-7	27		
44388.780	0.076		10	-42	35		
44390.875	0.120	60	45	-34			
44739.900	0.418	-57		2	51		
44740.830	0.438	-43	80	-38	2		
44744.820	0.521			-79	-38	43	
44895.510	0.672	-118	-57	-93	-74		
44897.520	0.714	-188	-171	-102	-44	160	
44898.520	0.735	-226	-60	-113	-106		
45067.880	0.276	-4		11	38	-47	
45068.890	0.297	-5	87	33	42	-128	
45069.910	0.319		79	46	88		
45070.910	0.339	-27	73	-9	20	-103	
45123.840	0.446	88		-10	30		
45184.640	0.718	-183		-110	-47		
45186.590	0.758	-190		-142	-88		
45189.610	0.821			-96	-63		
45190.600	0.842		-71	-125	-67		
45191.620	0.863	-65	-166	-65	-49		
45192.630	0.885	-208	-109	-79	-16		
45196.630	0.968	-51	-76	-77	-24		
45197.670	0.990	-59	57	-78	-19		
45198.640	0.010	-79	80	-53	11		
45199.630	0.031	-29	29	-16	9		
45248.520	0.053	-25	55	-35	25		-221:
45249.520	0.074	36	121	21	43	-46	
45250.510	0.095	83	64	76	86	-115	
45251.540	0.116	93	80	-1	68		12
45252.540	0.137	9	37	40	66	-80	-27
45254.530	0.179	84	131	-17	30		
45255.530	0.200	58	-17	-12	23		-72
45256.530	0.221	139	96	76	113		

Table 1 Continued

HJD	Phase ¹	N IV em. λ_0 4057.76	N V em. λ_0 4603.73	C III em. λ_0 4648.83	He II em. λ_0 4685.68	H γ abs. λ_0 4340.47	H β abs. λ_0 4861.33
2 400 000+							
45257.540	0.242		-26	74	102		
45258.530	0.263		16	21	48		
45260.530	0.304	-5	99	50	29		-67
45502.750	0.369		113	-34	36		
45506.840	0.455	68	-13	5	62		
45507.830	0.475	0	37	-19	40		
45508.780	0.495		-31	-11	24	6	92
45555.670	0.476	10	-57	-39	4		
45846.750	0.562	12	7	-61	-37		206:
50536.880	0.631	-120	-51	-103	-41	116	88
50537.883	0.652	-123	-133	-109	-53		
50538.872	0.672	-124	-118	-112	-34		118
50539.886	0.693	-125	-104	-122	-78		39
50540.878	0.714	-176	-144	-130	-55		86
50541.882	0.735	-130	-143	-136	-59		
50542.877	0.756	-169	-141	-100	-70		144
50858.851	0.363	-38	50	-34	26	-24	-120
50860.844	0.404	-45	5	-47	15	-47	-124
51261.900	0.790	-93	-61	-121	-41		
51261.913	0.791	-125		-125	-38		
51264.909	0.853	-106	-75	-122	-49		
51266.907	0.895	-96	-4	-104	-31		
51267.901	0.916	-37	-28	-91	-34		39
51303.768	0.666	-102	-126	-105	-47	50	135
51304.820	0.688	-192		-112	-41		
51305.814	0.709	-160	-136	-119	-46		184
51653.819	0.985	-86	-17	-68	17		-15
51654.833	0.006	-69	-37	-56	12		47
51806.573	0.179	134	110	8	110		-191
51807.534	0.199	87	66	29	81	-68	-189
52009.863	0.430	-5	-14	-27	47	-57	-74
52010.898	0.452	-21	-22	-2	42		-7

Table 1 Continued

HJD	Phase ¹	N IV em. λ_0 4057.76	N V em. λ_0 4603.73	C III em. λ_0 4648.83	He II em. λ_0 4685.68	H γ abs. λ_0 4340.47	H β abs. λ_0 4861.33
52011.880	0.472	-15	-15	-41	37	42	
52192.503	0.249	51	36	18	52		-169
52193.496	0.270	69	90	29	83		-68
52194.503	0.291	66	69	16	64		-97
52195.501	0.312	52	73	7	59		-161

¹ Phases were computed according to $T_0 = 2,445,676.4+47.825E$ (See below).

3 Results and Discussion

3.1 The spectrum

The blue optical spectrum of WR 98 is illustrated in fig 1, with identifications for main spectral features. As seen in fig 1, the spectrum of WR 98 is dominated by emission lines of NIII, NIV, HeII, HeI, with a strong CIII feature at λ 4650Å, consistent with the WN-WC classification originally proposed by Smith (1968). All of HeI emission lines in our blue spectra show P-Cygni profiles, as well as HeII 5411Å and NIV 5203Å (See Fig. 1). Relative intensities of NIII, HeII, NIV, and CIII lines in our spectra of WR 98 indicate a spectral type WN7-8/C. No hydrogen is detected in the spectrum. Relative intensities of emission lines in the spectrum of WR 98 show no appreciable changes in the whole of our dataset spanning 20 years of observations.

We have compared the spectrum of WR 98 with that of stars classified as WN7o and WN8o (Smith et al. 1996), namely WR 55 and WR 123, for which we also have digital spectra observed with the same instrumental configuration as WR 98. This comparison indicates that WR 98 has a higher ionization degree than the WN8o star, because NIV emission lines in the spectrum of WR 98 are stronger and NIII emission lines are weaker. Actually, the WN spectrum of WR 98 mostly resembles that of WR 55, classified as WN7 by Smith et al. (1996). Thus our blue optical spectra of WR 98 would be best described as WN7o/WC. Fig. 2 shows the spectra of WR 123, WR 98, and WR 55 for comparison.

Several faint absorption lines were detected upon the WN emission lines in our spectra of WR 98. These absorptions are H γ and H β , HeI $\lambda\lambda$ 4026, 4471, and 5015 Å and HeII $\lambda\lambda$ 4200, and 4540Å. As will be shown below, these lines belong to an OB companion. Because HeII absorptions appear fainter than HeI in the OB spectrum, we presume that the companion probably is of

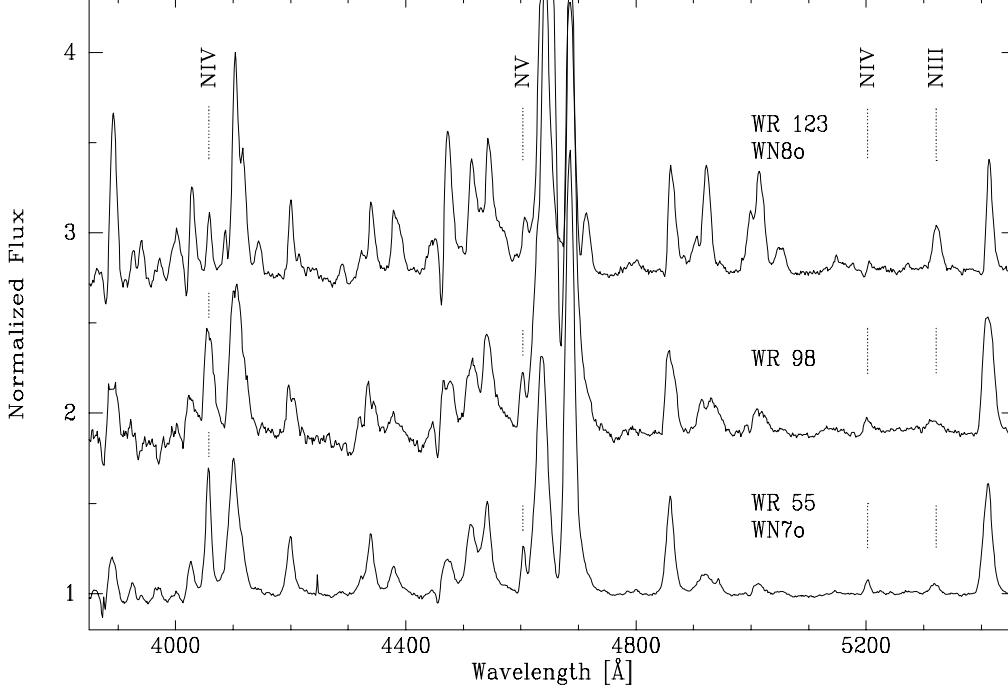


Fig. 2. Continuum normalized spectra of WR 123 (WN8o), WR 98, and WR 55 (WN7o). Note the similarity of the WN spectrum of WR 98 with that of WR 55.

3.3 The radial velocity orbit

Orbital elements for each emission line and the $H\gamma$ and $H\beta$ absorptions were determined with an improved version of the program originally published by Bertiau & Grobбен (1968). With the present data, the orbits of the four emission lines, NIV, NV, CIII, and HeII have negligible eccentricity, thus we have fitted circular orbits for all our radial velocities. Circular orbital elements for the individual lines are listed in Table 3.3, where V_0 refers to the center-of-mass velocity, K , to the semi-amplitude of the radial velocity variations, and T_0 is the time when the WR star is in the front of the system.

In our orbital fits the three best defined emission lines gave equal T_0 values within errors, therefore we adopt as ephemeris for the WR 98 binary system:

$$T_0 = 2,445,676.4 + 47.825E$$

NIV, NV, CIII, and HeII emission lines move in phase, indicating that they are formed in the same stellar envelope. This is also the case in the two other known WN/C binaries, namely WR 145 (MR 111) and WR 153 (GP Cep) (Massey & Grove 1989). No detectable phase delays among emission lines are present within the errors of the orbital fits.

Semi-amplitudes of the orbital motion of the HeII and CIII emission lines appear lower than those of ionized Nitrogen emission lines. This effect is also

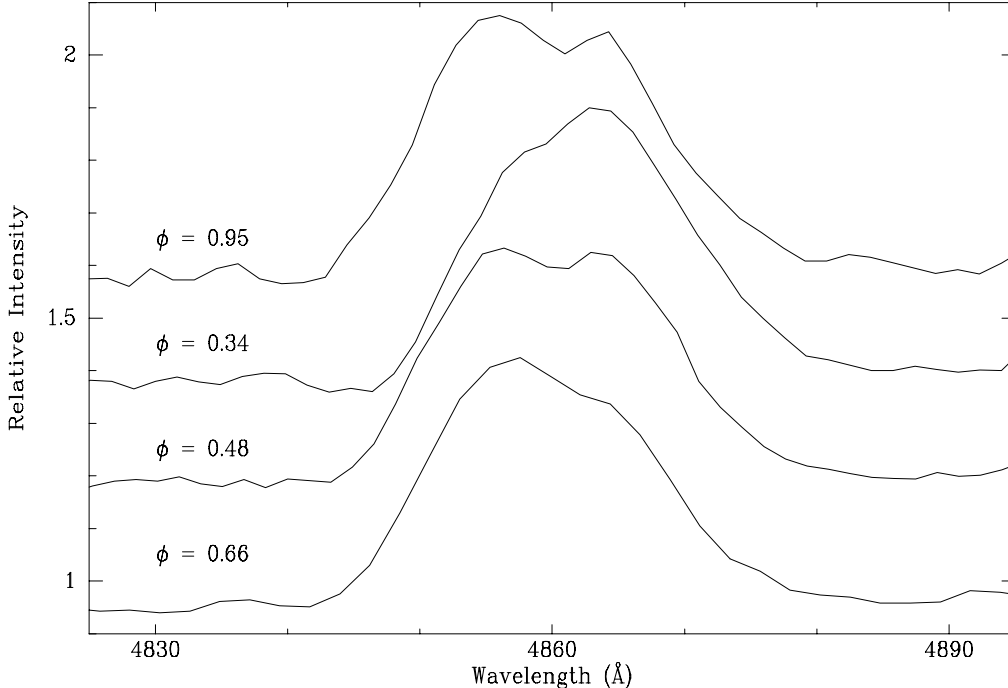


Fig. 3. Continuum rectified spectra of the HeII 4859Å emission with the superimposed H β absorption observed during four different phases of the binary system. Note the antiphased movement of absorption and emission. The spectra are intensity-shifted for a better presentation.

observed in other WR binaries, e.g. WR 29 (Niemela & Gamen 2000), and may arise if the HeII and CIII lines are partly formed in the interaction region of the binary components.

We measured H γ and H β absorptions in those spectra of WR 98 where this was possible. Radial velocities of these hydrogen lines phased with the binary period move anti-phased with the emission lines, thus indicating that they belong to an O type companion of the WR component in the binary system. Fig. 3 depicts the behaviour of the H β absorption line upon the HeII 4859 Å emission in four different binary phases, illustrating the antiphased movement of the absorption and emission lines.

The circular orbital elements for the hydrogen absorption lines are included in Table 3.3, and depicted in Fig 4.

The orbital semi-amplitudes of the radial velocity variations of the absorption lines and of NIV, NV, HeII and CIII emission lines indicate mass-ratios ($\mathcal{M}_{WR}/\mathcal{M}_O = q$) between 1 and 1.8. If a monotonic outward decreasing temperature gradient exists in the expanding WR envelope, we expect that the highest ionization emission, namely NV, represents better the orbital motion of the WN/C component, thus a value of $q \sim 1$ seems more plausible. However, taking into account the rather high uncertainties in the radial velocity

Table 2
Circular Orbital Elements of WR 98

Parameter	WN/C				OB
	N IV em.	N V em.	C III em.	He II em.	absorptions
P [days]	47.825 ± 0.005				
V_0 [km s^{-1}]	-41 ± 4	-15 ± 3	-47 ± 2	4 ± 2	6 ± 15
K [km s^{-1}]	106 ± 6	109 ± 5	72 ± 3	65 ± 3	112 ± 16
T_0 [HJD] ^(*)	6.4 ± 0.5	5.5 ± 0.4	6.5 ± 0.3	6.3 ± 0.3	
$a \sin i$ [R_\odot]	100 ± 5	103 ± 5	68 ± 3	61 ± 3	106 ± 15
$\mathcal{M}_{WN} \sin^3 i$ [\mathcal{M}_\odot]	27 ± 10	28 ± 10	19 ± 8	18 ± 7	
$\mathcal{M}_{OB} \sin^3 i$ [\mathcal{M}_\odot]	25 ± 7	27 ± 7	12 ± 3	10 ± 3	
q	1.06	1.03	1.56	1.72	

* HJD 2,445,670+: Time of conjunction, the WN star in front of the system.

values of the absorption lines, these mass-ratios should not be overinterpreted. Values of minimum masses and q for both components are tabulated for each emission line in Table 3.3.

We also estimated the radii of the critical Roche lobes using the expression given by Paczynski (1971), which resulted $r_{RL} \sin i = 79.5 R_\odot$ for both components. Each component of the WR 98 binary system seems to be well inside its critical Roche radius.

3.4 The radial velocity analysis of P-Cygni absorption lines

We analysed the radial velocities of the three strongest P-Cygni absorption lines in our spectra of WR 98, namely He I 3888Å, 4471Å, and 5015Å. As the He I 3888Å absorption presents a rather asymmetric profile, we measured the barycenter of this line. Because He I 5015Å was not observed in the wavelength range of the photographic spectra, the radial velocities of this line were only determined in the digital spectra. The three P-Cygni absorption lines follow the orbital motion of the WN/C component of the binary, as illustrated in Fig 5.

Circular orbits were fitted to the radial velocity variations of the P-Cyg absorptions. We obtained similar systemic velocities for the three absorption lines: $v_0 \sim -1130 \pm 15 \text{ km s}^{-1}$. This systemic velocity could be considered as a lower limit of the terminal velocity of the WR stellar wind, and in fact the

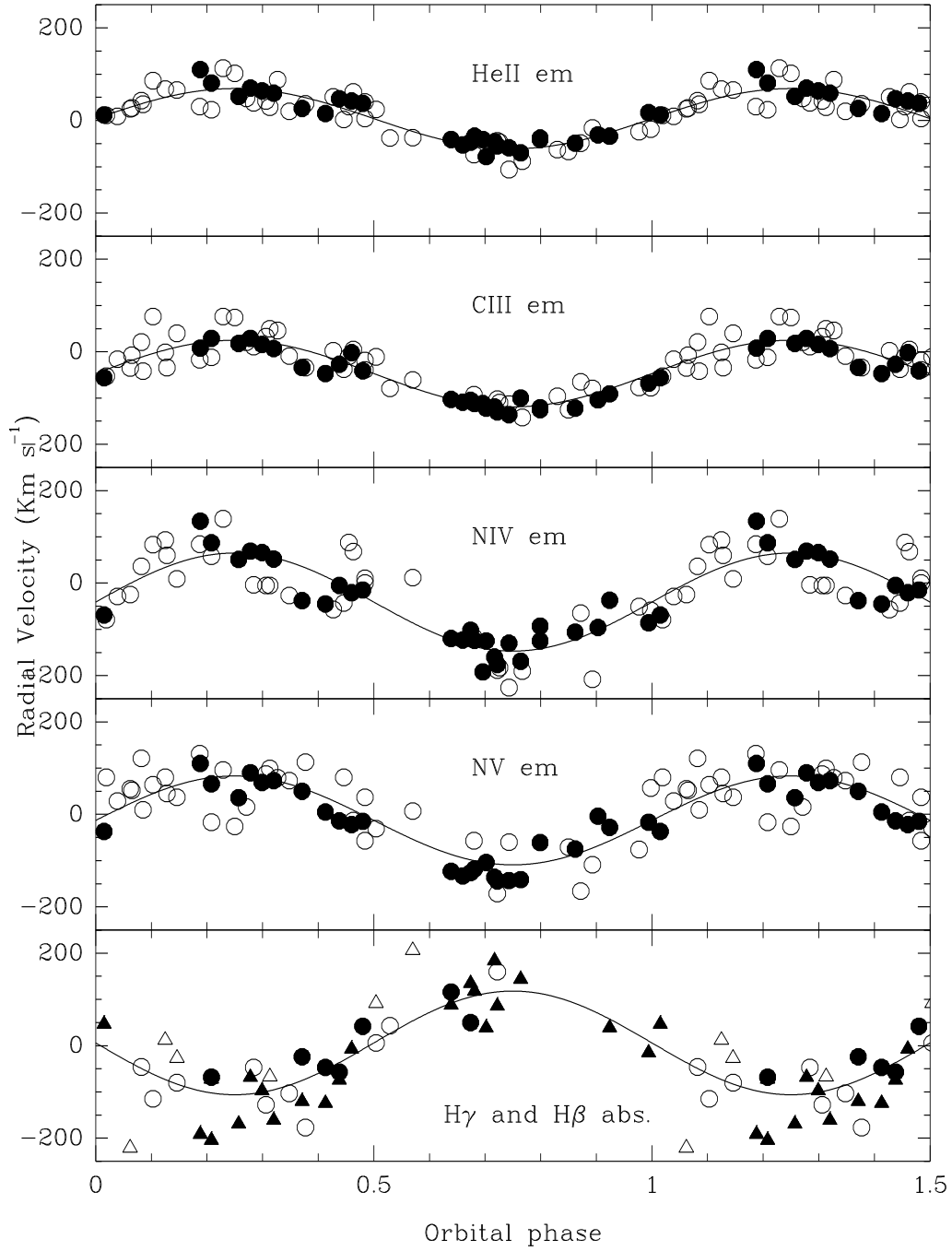


Fig. 4. Radial Velocities of HeII, CIII, NIV, and NV emission lines, and $\text{H}\gamma$ (circles) and $\text{H}\beta$ (triangles) absorption lines phased with the ephemeris $2,445,676.4+47.825\text{E}$. Open symbols represent the photographic data, and solid symbols, the digital CCD data. Curves are the orbital solutions from Table 3.3.

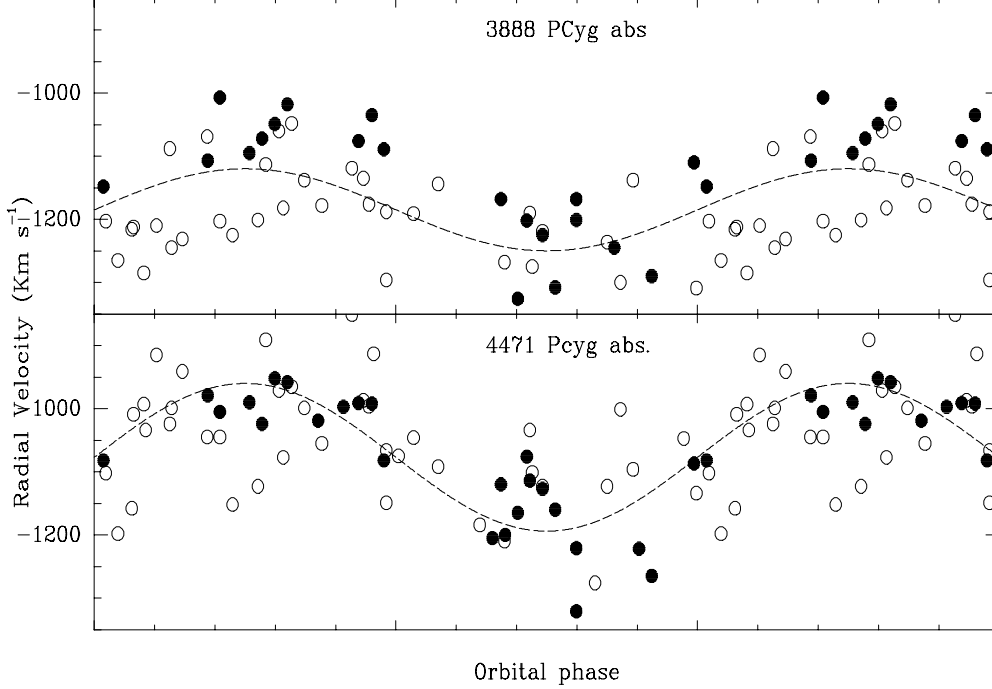


Fig. 5. Variations of the radial velocities of two He I P-cygni absorption lines in the spectrum of WR 98, symbolized and phased with the same ephemeris as emission lines in Fig. 4. Dashed lines represent circular orbital solutions.

value agrees with the determination of terminal wind velocity of WR 98 by Eenens & Williams (1994).

Semi-amplitudes of the radial velocity variations of the P-Cyg absorptions gave different values, namely 65 and 104 $km\,s^{-1}$ for He I $\lambda\lambda$ 3888, and 4471 and 5015Å respectively. The lower semi-amplitude of the orbital motion of He I 3888Å could be indicating that this line has another component, possibly originating in a common expanding envelope surrounding the binary, and which is not possible to deblend in our spectra. Similar behavior of He I λ 3888Å low-energy metastable absorption line is observed in the spectra of other WR binary stars, e.g. HD 214419 (= WR 155) (See Leung et al. 1983).

4 Conclusions

Our radial velocity analysis of lines in the spectrum of WR 98 based on a long term spectroscopic database confirms that this star is a binary system with a period of 47.825 days. Nitrogen and Carbon emission lines in the spectrum move in phase, which indicates that they are formed in the same stellar envelope.

We have detected faint absorption lines upon the WR emissions in our spectra.

These absorptions belong to an O-type component of the binary, with orbital motion anti-phased with the WR emissions. Thus, WR 98 is one more member of the very limited sample of WR+OB double-lined binaries, the first one with a WR component which appears to be at an intermediate evolutionary phase between the WN and WC stages.

The minimum masses indicated by our radial velocity orbit are quite high. Adopting the radial velocity orbit of the Nv emission as representative of the motion of the WR component of the binary, we obtain values of minimum masses of 28 and 27 M_{\odot} for the WR and OB components, respectively. Therefore, the component which at present shows the WR type spectrum, must have been very massive during its main sequence stage. This is in agreement with the estimate of 80 M_{\odot} for the cluster turn-off of Tr 27 (Massey et al. 2001), of which WR 98 is a probable member.

A comparison of the WN spectrum of WR 98 with other stars classified as WN8o (WR 123) and WN7o (WR 55), shows a remarkable resemblance of WR 98 with the WN7o spectrum, as seen in the Fig. 3. In our data, the classification of WR 98 as WN7/C appears more likely.

P-Cygni absorption lines of HeI in our spectra of WR 98 also follow the orbital motion of the WR component of the binary, thus these lines are formed in the expanding atmosphere of the WR star. We determined a systemic velocity of the P-Cyg absorptions of $\sim -1130 km s^{-1}$ for WR 98, which is in good agreement with the value of the terminal wind velocity published by Eenens & Williams (1994).

Acknowledgements

We are indebted to Federico Bareilles for his support in computer facilities. We thank the Directors and staff of CTIO and CASLEO for the use of their facilities. The CCD and data acquisition system at CASLEO has been partly financed by R.M. Rich through U.S. NSF Grant AST-90-15827. This research was supported in part through IALP-CONICET, Argentina.

References

- Abbott, D. C., Biegging, J. H., Churchwell, E., Torres, A. V. 1986, ApJ, 303, 239
- Bertiau, F. & Grobben, J. 1968, Ric. Astr. Spec. Vat., 8, 1
- Cannon, A. J. & Mayall, M. W. 1938, Harvard Observatory Bulletin, 908, 20
- Cincotta, P. M., Mendez, M., & Nuñez, J. A. 1995, ApJ, 449, 231
- Conti, P. S., & Massey, P., 1989, ApJ, 337, 251
- Eenens, P. R. J. & Williams, P. M. 1994, MNRAS, 269, 1082

- Feinstein, C., Baume, G., Vazquez, R., Niemela, V., & Cerruti, M. A. 2000, AJ, 120, 1906
- van der Hucht, K. A. 2001, NewAR, 45, 135
- van der Hucht, K., Conti, P., Lundstrom, I., & Stenholm, B. 1981, Space Sci. Rev., 28, 227
- Leung, K.-C., Seggewiss, W., & Moffat, A. F. J. 1983, ApJ, 265, 961
- Lundström, I. & Stenholm, B., 1984, A&ASS, 56, 43
- Marchenko, S. V., Moffat, A. F. J., Eversberg, T., Morel, T., Hill, G. M., Tovmassian, G. H., & Seggewiss, W. 1998, MNRAS, 294, 642
- Marraco, H. G. & Muzzio, J. C. 1980, PASP, 92, 700
- Massey, P., and Grove, K. 1989, ApJ, 344, 870
- Massey, P., DeGioia-Eastwood, K., and Waterhouse, E. 2001, AJ, 121, 1050
- Niemela, V. & Gamen, R. 2000, A&A, 362, 973
- Niemela, V. S. 1991, in K. A. van der Hucht & B. Hidayat (eds.), Wolf-Rayet Stars and Interrelations with Other Massive Stars in Galaxies, Proc. IAU Symp. 143, 201
- Paczynski, B. 1971, Ann. Rev. Astron. Astrophys., 9, 183
- Smith, L. F. 1968, MNRAS, 138, 109
- Smith, L. F., Shara, M. M., & Moffat, A. F. J. 1996, MNRAS, 281, 163